Carbohydrate Polymers 87 (2012) 265–273

Contents lists available at ScienceDirect

Carbohydrate Polymers

journal homepage: www.elsevier.com/locate/carbpol

A multitechnique approach to assess the effect of ball milling on cellulose

R. Avolio[a], I. Bonadies[a], D. Capitani[b], M.E. Errico[a], G. Gentile[a,*], M. Avella[a]

[a] Institute of Polymer Chemistry and Technology (ICTP), National Research Council (CNR), Via Campi Flegrei, 34-80078 Pozzuoli (Na), Italy
[b] Magnetic Resonance Laboratory "Annalaura Segre", Institute of Chemical Methodologies (IMC), National Research Council (CNR), Research Area of Rome, Via Salaria Km 29.300, 00016 Monterotondo Scalo (RM), Italy

ARTICLE INFO

Article history:
Received 9 May 2011
Received in revised form 14 June 2011
Accepted 25 July 2011
Available online 3 August 2011

Keywords:
Cellulose
Ball milling
Crystallinity
Morphology

ABSTRACT

This paper presents a detailed analysis of effect induced by a dry ball milling process on cellulose structure, morphology and properties. The partial amorphization of cellulose was qualitatively estimated by ATR-FTIR analysis. Through WAXD analysis the crystallinity index and the mean size of the cellulose crystallite domains were calculated, both these parameters showing a progressive decrease as a function of the milling time. In particular, crystallinity index decreased from 0.53 to 0.15 after 60 min ball milling, whereas the mean size of the cellulose crystallite domains showed a reduction from the original value of about 4.0 nm up to about 3.4 nm after 30 min. These quantitative results were confirmed by ^{13}C CP-MAS NMR analysis and measurements of the proton spin-lattice relaxation time in the rotating frame ($T^{1H}_{1\rho}$). Moreover, the increasing of the amount of water absorbed by cellulose samples (from 7.3 wt% for untreated cellulose up to 11.6 wt% for the cellulose sample ball milled for 60 min) and the reduction of the thermal stability were evaluated by TGA. Finally, SEM analysis revealed that the original fibrous structure almost disappeared and was modified to a quasi-circular shape.

1. Introduction

Cellulose has been recently defined as the most fascinating biopolymer with impressive structure and properties (Klemm, Heublein, Fink, & Bohn, 2005). It represents about 1.5×10^{12} tons of the total annual biomass production, and is considered an almost endless source of sustainable raw material for the even increasing demand for environmentally friendly and biocompatible products (Kaplan, 1998).

From a chemical point of view, cellulose is a carbohydrate polymer generated from repeating β-D-glucopyranose molecules that are covalently linked through acetal functions between the equatorial OH group of C4 and the C1 carbon atom (β-1,4-glucan). As a result, cellulose is a linear-chain polymer with three hydroxyl groups per anhydroglucose unit (AGU), with a degree of polymerization (DP) varying in a wide range depending on the origin and treatments. Cellulose from cotton and other plant fibres shows DP values in the 800–10,000 range.

From a structural point of view, cellulose is a semycrystalline material, whose crystallinity X_c can vary between 40 and 60%, although cellulose nanorods and cellulose deriving from other sources such as bacteria and tunicin show higher crystallinity values (Klemm et al., 2011). The crystalline phase is usually present in the I_α (triclinic unit cells) and I_β (monoclinic unit cells) modifications (Finkenstadt & Millane, 1998; Sugiyama, Vuong, & Chanzy, 1991). The cellulose polymorph composition reflects its origin and treatments (Atalla & Van der Hart, 1984).

Although very usual, cellulose I is thermodynamically less stable than other crystal structures, such as cellulose II, III, and IV (Klemm, Philipp, Heinze, Heinze, & Wagenknecht, 1998). Amongst these last, cellulose II is the most technically relevant form, and it is obtained from cellulose I by alkali treatment (mercerisation) or by cellulose dissolution followed by precipitation/regeneration. Cellulose II shows a monoclinic crystal structure with two antiparallel chains in the unit cell and a modified H-bonding system with respect to I_α and I_β crystal structures (Langan, Nishiyama, & Chanzy, 2001).

In the last years high energy ball milling (HEBM) has been proved to be a powerful tool to induce crystal structure modification of several materials, such as metals and alloys (Weeber & Bakker, 1988), polymers (Bai, Spontak, Koch, Saw, & Balik, 2000) and low molecular weight organic substances (Willart & Descamps, 2008). Ball milling has been also used to induce structural changes of cellulose either in wet and dry conditions. In dry conditions it has been able to significantly increase the cellulose amorphous content (Maier, Zipper, Stubicar, & Schurz, 2005), whereas wet ball milling with different relative amount of water has been able to transform native cellulose I to cellulose II (Ago, Endo, & Hirotsu, 2004). Ball milling of cellulose in the presence of different solvents has been also studied (Ago, Endo, & Okajima, 2007). Recently, thermal properties of dry ball milled cellulose and re-crystallization processes undergone in various relative humidity (RH) conditions have been investigated (Paes et al., 2010). Finally, the effect of ball milling on the hydrolysis

* Corresponding author. Tel.: +39 081 8675057.
E-mail address: gennaro.gentile@ictp.cnr.it (G. Gentile).

0144-8617/$ – see front matter © 2011 Elsevier Ltd. All rights reserved.
doi:10.1016/j.carbpol.2011.07.047

of microcrystalline cellulose in hot-compressed water and in dilute acid solutions has been also reported (Zhao et al., 2006).

Nevertheless, a systematic research work in which different properties of dry ball milled cellulose are deeply evaluated and compared is still necessary.

Cellulose fibres deriving from wood pulp have been investigated. They are commercialised as fillers for several applications, including the fabrication of green composites. In this field, the employment of an amorphous cellulose can be very interesting to impart specific functional properties to the materials, such as a tunable biodegradability kinetics.

On these bases, the effect of a dry ball milling process on cellulose structure and properties was investigated in this work through a multitechnique approach. In this way, it was possible to unambiguously relate the expected amorphization and other critical morphological physical and structural properties of ball milled cellulose, before using it for specific applications.

2. Experimental

2.1. Preparation of ball milled cellulose samples

Cellulose fibres were Arbocel® BWW40, kindly supplied by JRS (Rosenberg, Germany). The declared average length of the fibres is 200 μm, the average fibre diameter is 20 μm. Before milling, cellulose fibres were dried at 90 °C under vacuum for 24 h. Therefore cellulose samples of 10.0 ± 0.1 g were milled in a Retsch PM100 planetary ball milling system (Haan, Germany), using a 125 mL steel milling cup and 25 spheres, 10 mm diameter. The weight ratio spheres/cellulose was about 10:1. The ball milling process was carried out for 2, 4, 8, 15, 30 and 60 min.

2.2. Characterizations

Attenuated Total Reflectance Fourier-Transform InfraRed (ATR-FTIR) spectroscopy analysis was carried out on neat and ball milled cellulose samples on a Perkin Elmer Spectrum One FTIR spectrometer (Wellesley, MA, USA), equipped with the Universal ATR accessory, using 64 scans and a resolution of 4 cm^{-1}, over the range 4000–700 cm^{-1}. Before the analysis, samples were dried at 90 °C under vacuum for 24 h. Post-analysis manipulation of spectra was kept to a minimum. Cellulose spectra were baseline-corrected so that the minimum between 2000 and 1800 cm^{-1} was set equal to zero and they were normalized as below described.

Wide angle X-Ray Diffraction (WAXD) analysis was carried out on untreated and ball milled cellulose samples by means of a Philips powder diffractometer PW 1050 (PANalytical B.V., Almelo, The Netherlands) equipped with a rotating sample-holder device, using a Ni-filtered CuKα radiation (wavelength 1.5418 Å). Measurements of the diffracted intensities were performed in the range of 3–60° (2θ), at room temperature and at a scanning rate of 1°/min. Before the analysis, samples were conditioned at 25 °C and 50% RH for 48 h.

Thermogravimetric analysis (TGA) was carried out using a Perkin Elmer Pyris Diamond thermogravimetric analyser (Wellesley, MA, USA). Measurements were performed on neat and ball milled cellulose samples previously conditioned at 25 °C and 50% RH for 48 h. About 10 mg of each sample were analysed at a heating rate of 10 °C min^{-1} in nitrogen flux (50 NmL min^{-1}).

Morphological analysis was performed using a FEI Quanta 200 FEG environmental scanning electron microscope (ESEM) (Eindhoven, The Netherlands) in low vacuum mode, using a Large Field Detector (LFD) and an accelerating voltage ranging between 15 and 20 kV. Before the analysis, dried cellulose samples were mounted on aluminium stubs by means of carbon adhesive disks.

Solid state ^{13}C CP-MAS NMR spectra were collected at 100.47 MHz on a Bruker Avance II 400 spectrometer operating at a static field of 9.4 T, equipped with a 4 mm MAS probe. Neat and ball milled cellulose samples were packed into 4 mm zirconia rotors and sealed with Kel-F caps. The spinning speed was set at 8 kHz for all NMR experiments. Spectra were acquired with a contact time of 1.5 ms. The ^1H $\pi/2$ pulse width was 2.80 μs, 10,000 scans were collected. The cross-polarization was performed applying a variable spin-lock sequence RAMP-CP-MAS (Alexander, 1969; Shezad, Khan, Khan, & Kon Park, 2010). Spectra were obtained using 1024 data points in the time domain, zero-filled and Fourier transformed.

$T_{1\rho}^{1H}$ measurements were performed indirectly by varying the duration of the ^1H spin-lock period (τ) before applying ^1H–^{13}C cross polarization (CP) with a contact time of 1.5 ms. For each experiment, 17 spectra were collected with τ ranging from 0.1 up to 25 ms. For each spectrum, 2048 scans were collected. $T_{1\rho}^{1H}$ values were calculated fitting the experimental data to an exponential function:

$$M = M_0 + A \ \exp\left(\frac{-\tau}{T_{1\rho}^{1H}}\right) \quad (1)$$

Spectral deconvolution was performed using the software package Grams/8.0AI, THERMO Electron Corporation. A mixed Gaussian (95%) and Lorentzian (5%) line shape was chosen. Each resonance was characterized by the following parameters: amplitude, chemical shift and line width at half height.

3. Results and discussion

3.1. Energy transferred during the milling process

Several attempts have been made to model the ball milling process in order to estimate the energy transferred to materials (Abdellaoui & Gaffet, 1995; Dallimore & McCormick, 1996; Gaffet, 1991; Magini & Iasonna, 1995; Magini & Iasonna, 1996; Magini, Colella, Iasonna, & Padella, 1998; Maurice & Courtney, 1990). The transfers of mechanical energy inside a planetary ball mill occur via ball–ball and ball–vial wall collisions so that the simplest model used to describe the ball milling process is the kinematical one, based on the collision theory. According to this model the energy developed in a ball mill is a function of several variables such as the number of balls, the angular velocity of the plate of the mill and the milling time. Instead all the other parameters regarding the dimension of the mill, the vial and the balls are considered as geometrical parameters. Since the kinetic shock energy is not well defined, in order to simplify the problem the following assumptions are taken into account to perform the numerical calculations (Magini, Iasonna, & Padella, 1996; Murty, Mohan Rao, & Ranganathan, 1995):

- The ball and the inner vial wall are covered with a thin powder layer; in this case a ball transfers all its kinetic energy to the powder particle on impact (inelastic hits).
- The ball moves integral with the vial, without rolling or sliding on the inner wall, until it is launched at a given moment against the opposite wall by a given composition of inertial forces.
- The energy is only released by collisions between balls and wall.

Variables

N_b	number of balls = 25
PW	powder weight = 10 g
W_p	angular velocity of the plate = 650 rpm = 68.07 rad s^{-1}
t	milling time, variable [s]

Geometrical parameters

d_b	diameter of the ball = 10.0×10^{-3} m
m_b	weight of the ball = 4.00×10^{-3} kg

D_v diameter of the pot = 60.0×10^{-3} m
H_v height of the pot = 53.0×10^{-3} m
$R_p - R_v$ distances from the centre of the mill to the centre of the vial and from the centre of the vial to its periphery = 41.5×10^{-3} m
W_v absolute angular velocity of the vial = 136.1 rad s^{-1}

When one ball is launched from the inner wall to the opposite side it possesses the kinetic energy:

$$E_b = \frac{1}{2} m_b V_b^2 \tag{2}$$

V_b is the absolute velocity of a ball.

The effects of this energy are the deformation of the material entrapped between the ball and the wall, and the instantaneous rise of temperature of the system containing the ball, the region of the wall hit and the material entrapped. After a short succession of hits, during which decreasing fractions of energy are released, the residual energy of the ball becomes:

$$E_s = \frac{1}{2} m_b V_s^2 \tag{3}$$

V_s is the velocity of a ball after the succession of collisions (velocity inner wall).

Because the vial contains a finite number of balls N_b, that hinder each other, we have to introduce in the equation of the total energy an empirical factor, $\varphi_b = (1 - n_v^{\varepsilon})$ where ε and n_v are geometrical parameters correlated to the number of balls in the vial and the dimensions of the vial, able to account for the degree of filling of the vial in the equation of the total energy:

$$\Delta E_b^* = \varphi_b \Delta E_b \quad [\text{kg m}^2\,\text{s}^{-1}] \tag{4}$$

Introducing the theoretical expressions for the angular velocity and acceleration derived elsewhere (Burgio, Iasonna, Magini, Martelli, & Padella, 1991), the following relationship is obtained:

$$\Delta E_b = E_b - E_s = -m_b \left[\left[W_v^3 \frac{(R_v - (d_b/2))}{W_p} + W_p W_v R_p \right] \left(R_v - \frac{d_b}{2} \right) \right] \tag{5}$$

The total power transferred from the mill to the system during collisions can be expressed as:

$$P = \varphi_b \Delta E_b N_b f_b \quad [\text{kg m}^2\,\text{s}^{-3}] \tag{6}$$

where the frequency of collision is:

$$f_b = K \times \frac{(W_p - W_v)}{2} \times \pi \tag{7}$$

K is a constant related to the time necessary to dissipate the energy ΔE_b^*. It is equal to 1.5 for ball diameters ranging between 8 and 10 mm.

Therefore the total energy transferred from the mill to the system during collisions is:

$$P^* = Pt \quad [\text{kg m}^2\,\text{s}^{-2}]$$

that is, normalising by the weight of the powder:

$$P^* = \left(\frac{Pt}{KPW} \right) = -\varphi_b N_b m_b t (W_p - W_v) \times \left[W_v^3 \frac{(R_v - (d_b/2))}{W_p} + W_p W_v R_p \right] \frac{(R_v - (d_b/2))}{2\pi PW} \tag{8}$$

Using this equation it was possible to calculate the energy transferred during the milling process at different milling time.

As a result, P^* increases linearly with increasing the milling time, from a value of 6.29 kJ for a milling time of 2 min, up to a value of 188.80 kJ for the 60 min lasting milling process. This means that the energy transferred to cellulose during the milling process ranges from about 102 kJ per mol of β-D-glucopyranose units (2 min milling), up to about 3060 kJ per mol of β-D-glucopyranose units (60 min ball milling).

3.2. ATR-FTIR analysis

FTIR analysis is a very useful technique to monitor structural changes undergone by cellulose during chemical and mechanical treatments (Avella et al., 2007, 2008; Princi et al., 2006). Fig. 1 shows normalized ATR-FTIR spectra of neat cellulose and cellulose ball milled at different milling time in those regions in which relevant changes in the spectra were observed as a function of the milling time: wavenumber ranges 850–1190 (Fig. 1, region 1), 1190–1520 (Fig. 1, region 2) and 2800–3700 cm^{-1} (Fig. 1, region 3). Spectral normalization was based on the absorbance of the CH bending at 1375 cm^{-1}, expected to be almost insensitive to degradation/amorphization processes (Tomsic, Simoncic, Orel, Vilcnik, & Spreizer, 2007). Main FTIR assignments of cellulose and predicted IR band frequencies have been elsewhere reported (Barsberg, 2010; Schwanninger, Rodrigues, Pereira, & Hinterstoisser, 2004).

Several FTIR based methods have been proposed to characterize amorphous domains and amorphous/crystalline ratio in cellulose (Åkerholm, Hinterstoisser, & Salmén, 2004; Evans, Newman, & Roick, 1995; Hishikawa, Togawa, Kataoka, & Kondo, 1999; Kataoka & Kondo, 1998). The ratio between absorbance values of bands centred at about 1430 and 895 cm^{-1} (A_{1430}/A_{895}), and at 1372 and 2900 cm^{-1} (A_{1372}/A_{2900}) have been used as an evaluation of the crystallinity index (Kataoka & Kondo, 1998; Schwanninger et al., 2004). Unfortunately, FTIR based methods are not absolute measurement techniques. In the case of the ratio A_{1430}/A_{895}, for instance, a non linear relationship between the IR and the X-ray crystallinity index has been found (Kataoka & Kondo, 1998). Furthermore, the absorbance values of these bands are affected by other bands of the cellulose spectrum.

In our case, main changes are observed for the absorption bands centred at 1024, 1052, 1112, 1320, 1337 and 1431, 2900 and in the range from 3200 to 3500 cm^{-1}. In particular, bands at 1112, 1320, 1337 and 1431 cm^{-1} seem to be very sensitive to the ball milling process and after 60 min lasting ball milling, these bands tend to disappear, thus indicating a progressive pronounced reduction of the cellulose crystallinity during the process.

Finally, it is to be remarked that no evidences of oxidization phenomena have been observed in the whole spectral region as a consequence of the ball milling treatment.

3.3. WAXD analysis

WAXD analysis was performed in order to evaluate structural changes undergone by cellulose as a function of the ball milling time. As it is shown in Fig. 2, curve a, the WAXD intensity profile collected for untreated cellulose exhibits the well resolved spectrum of Cellulose I (Segal, Creely, Martin, & Conrad, 1962) with the three characteristic reflections (1 0 1), (1 0 $\bar{1}$) and (0 0 2). The first two reflections, of medium-strong intensity and highly convoluted each other, are obtained with 2θ ranging between 13 and 18° and the third, almost totally resolved, very sharp and with a very strong intensity, is obtained for a 2θ value of 22.6°. Moreover, another peak, of weak intensity, characteristic of the (040) reflection, can be observed at a 2θ value of 34.7°.

From Fig. 2, it can be underlined that typical Cellulose I profiles are shown also by ball milled cellulose samples although these profiles become less resolved with increasing the ball milling time. After 60 min ball milling (profile g) the characteristic shape of the cellulose I crystal structure is completely lost. Crystallinity index

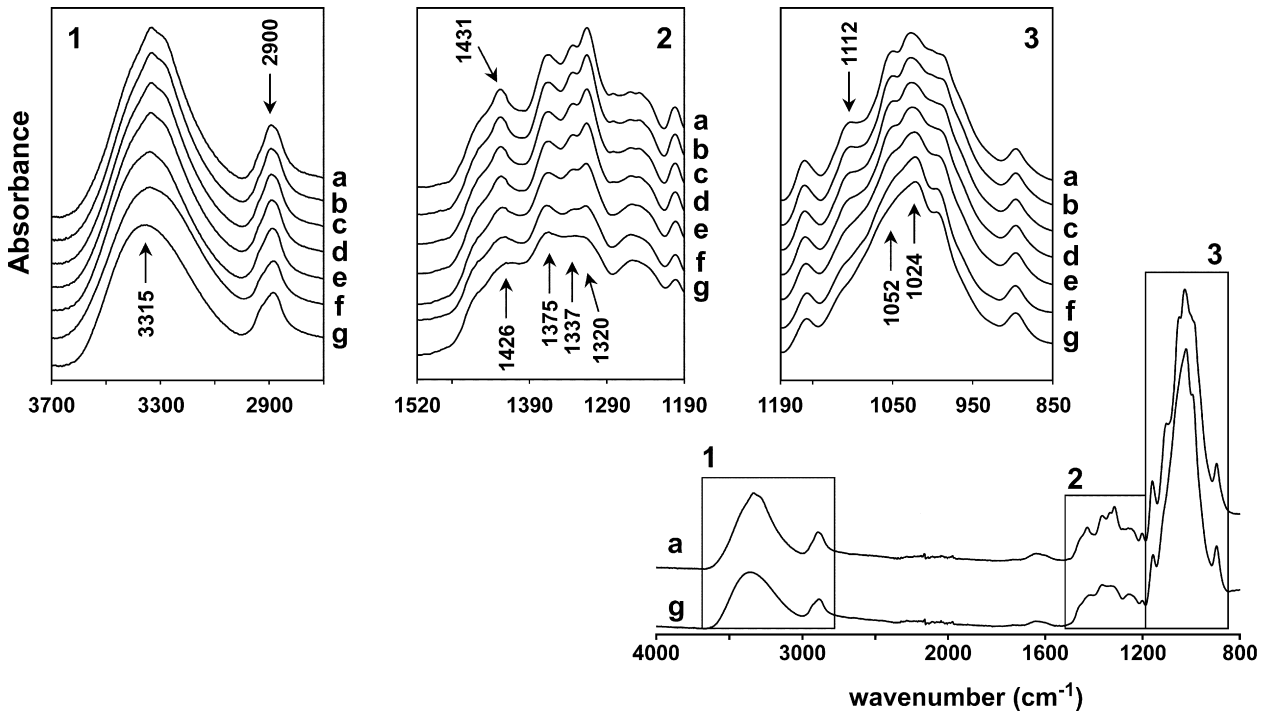

Fig. 1. ATR FTIR spectra of cellulose samples: (a) untreated; ball milled for: (b) 2 min; (c) 4 min; (d) 8 min; (e) 15 min; (f) 30 min; (g) 60 min.

values (X_c) were obtained through the amorphous subtraction method (Park, Baker, Himmel, Parilla, & Johnson, 2010; Segal et al., 1962; Thygesen, Oddershede, Lilholt, Thomsen, & Ståhl, 2005):

$$X_c = \frac{A_T - A_{AM}}{A_T} \quad (9)$$

where A_T is the total area under the WAXD intensity profile and A_{AM} is the area of the amorphous cellulose sample, whose shape was obtained by a Gaussian fit of the intensity profile of cellulose sample ball milled for 60 min. As resumed in Table 1, the progressive amorphization of cellulose with the ball milling time is evident.

Another parameter useful to evaluate the structural changes of cellulose during ball milling is the mean size of the cellulose crystallite domains, D, that can be obtained according to the Scherrer equation (Alexander, 1969):

$$D = \frac{k\lambda}{\beta \cos\theta} \quad (10)$$

where k is a shape factor whose value can be approximated to 0.89 (Shezad et al., 2010), although it varies with the shape of the crystallites, β is the line width in radians at half the maximum intensity of the reflection (0 0 2) to which the background and the amorphous component have been subtracted, λ is the wavelength of the radiation used (1.54 Å) and θ is the Bragg angle of the (0 0 2) peak. Average dimension of crystal domains varies from about 4 nm for untreated cellulose to 3.4 nm for cellulose ball milled for 30 min, whereas at 60 min ball milling the almost complete disappearance of the (0 0 2) peak prevents the calculation of D.

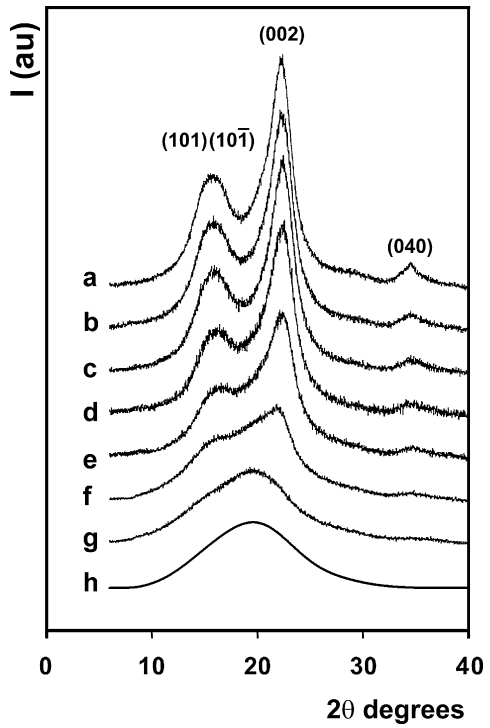

Fig. 2. WAXD intensity profiles of cellulose samples: (a) untreated; ball milled for: (b) 2 min, (c) 4 min, (d) 8 min, (e) 15 min, (f) 30 min, (g) 60 min; (h) amorphous halo.

3.4. Solid state ^{13}C NMR analysis

3.4.1. ^{13}C CP-MAS NMR analysis

Fig. 3 shows ^{13}C CP-MAS NMR spectra of untreated and ball milled cellulose samples. The deconvoluted spectra with all components used in deconvolutions are also shown. Besides the resonance of the anomeric carbon C1 centred at 104.7 ppm, other two weak resonances are observed in that range centred at 102 and 97 ppm respectively. These resonances, already observed in the starting material, see Fig. 5a, are ascribable to internal residues and reducing end of low molecular weight cellulose oligomers. It is noticeable that the intensity of these resonances slightly increases with the milling time, thus indicating the occurrence of a partial macromolecular chain scission. However, this phenomenon did not lead to a relevant decrease of the molecular weight since the amount

Table 1
Crystallinity index values (X_c), mean size of the cellulose crystallite domains (D) and $T_{1\rho}^{1H}$ values measured on resonances C4a and C6a belonging to amorphous, less ordered domains, and on resonances C4c and C6c, belonging to crystalline domains (R^2 values in brackets).

Sample	X_c[a] (±2.0%)	D (nm) (±0.05)	X_{C6}[b]	X_{C4}[c]	C4c (88.5 ppm) $T_{1\rho}^{1H}$ (ms)	C4a (82.9 ppm) $T_{1\rho}^{1H}$ (ms)	C6c (65.0 ppm) $T_{1\rho}^{1H}$ (ms)	C6a (63.0 ppm) $T_{1\rho}^{1H}$ (ms)
Cellulose	0.53	3.97	0.50	0.52	16.9 (0.979)	12.0 (0.991)	18.4 (0.980)	12.5 (0.994)
Cellulose BM 2 min	0.51	3.90	0.46	0.50	17.9 (0.996)	13.5 (0.991)	20.7 (0.971)	12.9 (0.999)
Cellulose BM 4 min	0.49	3.85	0.43	0.47	15.3 (0.987)	11.0 (0.996)	19.7 (0.974)	11.7 (0.986)
Cellulose BM 8 min	0.45	3.54	0.37	0.42	19.1 (0.985)	13.4 (0.993)	22.1 (0.959)	13.3 (0.998)
Cellulose BM 15 min	0.38	3.43	0.30	0.31	18.4 (0.984)	11.5 (0.989)	21.0 (0.987)	11.6 (0.997)
Cellulose BM 30 min	0.28	3.37	0.19	0.17	[a]	11.4 (0.992)	[a]	10.4 (1.000)
Cellulose BM 60 min	0.15	–	0.10	0.07	[a]	7.7 (0.986)	[a]	9.4 (0.998)

[a] X_c: crystallinity index calculated with the amorphous subtraction method (Eq. (9)).
[b] X_{C4}: crystallinity index calculated by NMR analysis using Eq. (11) and intensity of resonances C4a and C4c.
[c] X_{C6}: crystallinity index calculated by NMR analysis using Eq. (11) and intensity of resonances C6a and C6c.

of water soluble fractions recovered from neat and ball milled cellulose samples was comparable. Moreover, the absence of any resonance attributable to oxidized groups confirmed that no oxidation phenomena occur during the ball milling, in agreement with the results obtained by FTIR analysis.

The solid state ^{13}C CP-MAS spectrum of cellulose exhibits separable resonances from crystalline and from less ordered domains for C4 and C6 atoms in the anhydroglucose units. In fact resonances labelled with a "c", namely C4c and C6c at 88.5 and 65.0 ppm respectively, are assigned to cellulose in crystalline domains, whereas resonances labelled with an "a", namely C4a and C6a at 82.9 and 63.0 ppm respectively, are assigned to cellulose in disordered, amorphous domains. (Hult, Larsson, & Iversen, 2000; Larsson, Wickholm, & Iversen, 1997; Teeäär, Serimaa, & Paakkari, 1987).

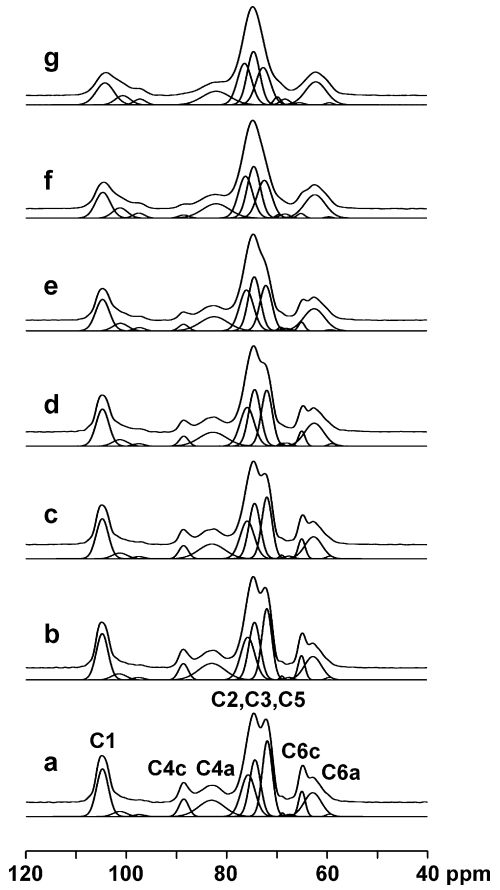

Fig. 3. ^{13}C CP-MAS NMR spectra of (a) cellulose (b) cellulose ball milled for 2 min, (c) 4 min, (d) 8 min, (e) 15 min, (f) 30 min, and (g) 60 min. The experimental spectra are shown along with the components obtained applying the deconvolution procedure.

In analyzing cellulose by NMR a crystallinity index X_{C4} may be defined as the crystalline fraction of cellulose in an investigated sample:

$$X_{C4} = \frac{I(C4c)}{I(C4c) + I(C4a)} \quad (11)$$

where I(C4c) and I(C4a) are the intensities of resonances C4c and C4a obtained applying a deconvolution procedure to experimental spectra. The crystallinity index X_{C6} may be also calculated using the intensities of resonances C6c and C6a. In Table 1 both indexes are reported. Note that, even applying a strong resolution enhancement, no split was observed in the resonance ascribed to C4a.

It is worth noting that the spectrum of the starting material shows a rather low index of crystallinity which was found to be about 0.50, see Table 1. As the duration of the ball milling process increases, the index of crystallinity progressively decreases indicating a progressive amorphization of the cellulose. After 60 min of ball milling the crystallinity index decreases down to about 0.07–0.10.

Fig. 4 reports the crystallinity index X_c obtained by X-ray analysis and indexes X_{C4} and X_{C6} obtained by NMR. All measurements show a progressive lowering of the crystalline content as the ball milling duration increases, up to 0.10 after 60 min ball milling (see Table 1), in good agreement with WAXD results.

3.4.2. Analysis of proton relaxation times in the rotating frame

The proton spin-lattice relaxation time in the rotating frame $T_{1\rho}^{1H}$ is sensitive to the motion of the proton spin system averaged by spin diffusion over a short distance. Actually it may be sensitive to macroscopic variations which may occur in the system under investigation.

$T_{1\rho}^{1H}$ values measured on starting cellulose and in cellulose ball milled at different lengths of time are reported in Table 1. In the

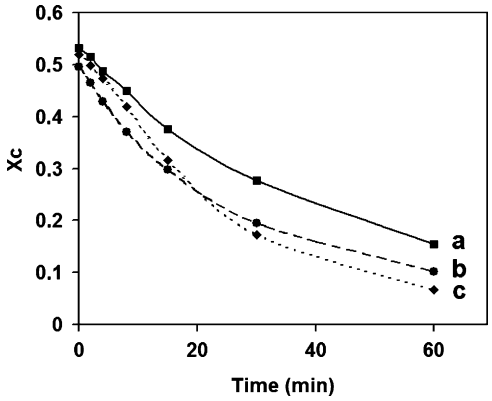

Fig. 4. Crystallinity index vs. ball milling time. (a) Crystallinity index calculated with the amorphous subtraction method, (b) by NMR using the intensity of resonances C6c and C6a, and (c) by NMR using the intensity of resonances C4c and C4a.

starting material values measured on resonances C4a and C6a assigned to cellulose in the amorphous domain are slightly shorter than C4c and C6c assigned to cellulose in the crystalline domain, indicating no great bias due to the local environment. It has been reported in the literature (Capitani, Proietti, Segre, & Ziarelli, 2002; Hori, Hirai, & Kitamaru, 1984) that in highly crystalline cellulose, $T_{1\rho}^{1H}$ value of resonance due to C4a was found to be about half of that measured for the resonance C4c, pointing out the low efficiency of the spin-diffusion process. Therefore the similar $T_{1\rho}^{1H}$ values we measured for resonances ascribed to C4c and C4a and to C6c and C6a, reveal that ^{1}H spin-diffusion partially averages out $T_{1\rho}^{1H}$ values of crystalline and amorphous domains. The spin diffusion path length L may be calculated using the following equation:

$$\langle L^2 \rangle = \left\langle \frac{T_{1\rho}^{1H}}{T_2} \right\rangle \langle L_0^2 \rangle \quad (12)$$

where L_0 is the distance between protons, about 0.1 nm, T_2 is the proton spin-spin relaxation time that below T_g is about 10 μs, and $\langle L^2 \rangle$ is the mean square distance over which magnetization is transported. As an example, considering $T_{1\rho}^{1H}$ values measured on resonances C6a and C6c, namely 12 and 17 ms, the spin-diffusion path length calculated according to Eq. (13) ranges between 3.5 and 4.2 nm. These data clearly indicate similar dimension in crystalline and amorphous domains. Besides, these data match well the dimension of domains obtained by X-ray analysis, see Table 1. After 60 min ball milling, $T_{1\rho}^{1H}$ values of amorphous components clearly shorten. The diffusive path length corresponding to a $T_{1\rho}^{1H}$ value of 8 ms is about 2.8 nm. The shortening of $T_{1\rho}^{1H}$ values along with the reduction of the diffusive path length are in accordance with the progressive amorphization of the cellulose structure and the reduction of domain dimension. Because resonances due to C6c and C4c became weaker and weaker as the ball milling time increases, at long ball milling times, namely 30 and 60 min, $T_{1\rho}^{1H}$ values of the crystalline phase could not be measured anymore, see Fig. 3f and g.

3.5. Thermogravimetric analysis

Thermogravimetric analysis in non oxidative conditions was used with the double aim of evaluating the amount of absorbed water and the cellulose thermal stability as a function of milling time.

In Fig. 5, the weight loss due to water desorption in the range 25–150 °C from untreated cellulose and ball milled cellulose samples is reported. As it can be observed, the amount of absorbed water increases with increasing the milling time, varying from 7.3 wt% for untreated cellulose up to 11.6 wt% for the cellulose sample ball milled for 60 min. This effect clearly depends on the crystal structure: as well stated, water can be easily absorbed by the amorphous fraction, whereas crystalline domains are less accessible to water molecules (Kocherbitov, Ulvenlund, Kober, Jarring, & Arnebrant, 2008).

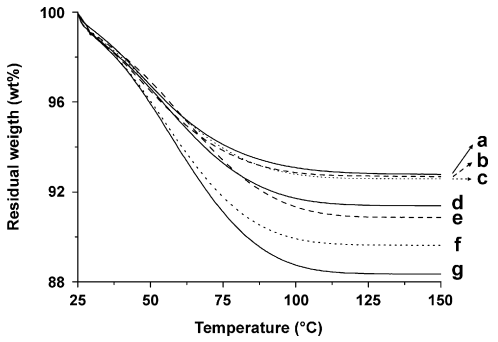

Fig. 5. Residual weight of cellulose samples during water desorption: (a) untreated cellulose; cellulose ball milled for: (b) 2 min, (c) 4 min, (d) 8 min, (e) 15 min, (f) 30 min, (g) 60 min.

Moreover, the ball milling process also influences the thermal stability of cellulose samples, slightly decreasing, especially at higher milling times, either the temperature of the onset of the decomposition (evaluated at 5 wt% of weight loss) either the temperature corresponding to the maximum degradation rate, both being found up to 12 °C lower than the corresponding temperature values shown by untreated cellulose (see Table 2). Although the decrease of degradation temperature values is not linear with increasing the amorphous content of the samples, also this effect can be ascribed to the crystallinity of cellulose samples because, before the degradation process starts, a significant amount of energy is required to disrupt crystalline domains (Avella et al., 2010; Pedersoli, 2000).

3.6. SEM analysis

From a qualitative point of view, SEM analysis of untreated and ball milled cellulose samples immediately revealed an extraordinary effect of the ball milling process on the shape of the fibres. A progressive reduction of the fibre length was observed increasing the milling time, and after 60 min of ball milling cellulose completely lost the fibrous structure and it was reduced to small particles with dimensions ranging in the micrometers. In Fig. 6 SEM micrographs at lower (A) and higher (B) magnification are reported, clearly showing the size reduction undergone by cellulose fibres during ball milling.

In order to quantify the effect of the ball milling process, SEM micrographs at low magnification were analysed by means of the public domain software ImageJ (release 1.43u) (Abramoff, Magelhaes, & Ram, 2004). For each sample, a minimum set of 5 low magnification micrographs was used for the image analysis. In particular, the average diameter and length

Table 2
Thermogravimetric and morphological analysis results. Weight loss due to water desorption (WL); temperature values corresponding to the onset of the decomposition process ($T_{5\,wt\%}$) and to the maximum degradation rate (T_{deg}); average length (L), average diameter (D) of the fibres, aspect ratio (AR) and circularity (C) for untreated and ball milled cellulose samples (standard deviation values in brackets).

Sample	WL (wt%)	$T_{5\,wt\%}$ (°C)	T_{deg} (°C)	L (μm)	D (μm)	AR = L/D	C
Cellulose	7.3	290	349	202 (45)	14.6 (4.4)	13.8	0.14 (0.03)
Cellulose BM 2 min	7.4	291	348	140 (53)	13.8 (5.1)	10.1	0.22 (0.08)
Cellulose BM 4 min	7.4	291	349	80 (69)	13.9 (4.0)	5.8	0.42 (0.20)
Cellulose BM 8 min	8.6	289	347	51 (35)	13.7 (4.5)	3.7	0.52 (0.15)
Cellulose BM 15 min	9.1	285	345	28 (20)	14.2 (4.2)	2.0	0.62 (0.16)
Cellulose BM 30 min	10.3	278	339	19 (15)[a]	10.4 (6.4)[b]	1.8	0.69 (0.16)
Cellulose BM 60 min	11.7	278	337	12 (8)[a]	7.8 (4.7)[b]	1.5	0.75 (0.15)

[a] Calculated as the average major axis of particles, whose shape was best fitted to an ellipse.
[b] Calculated as the average minor axis of particles, whose shape was best fitted to an ellipse.

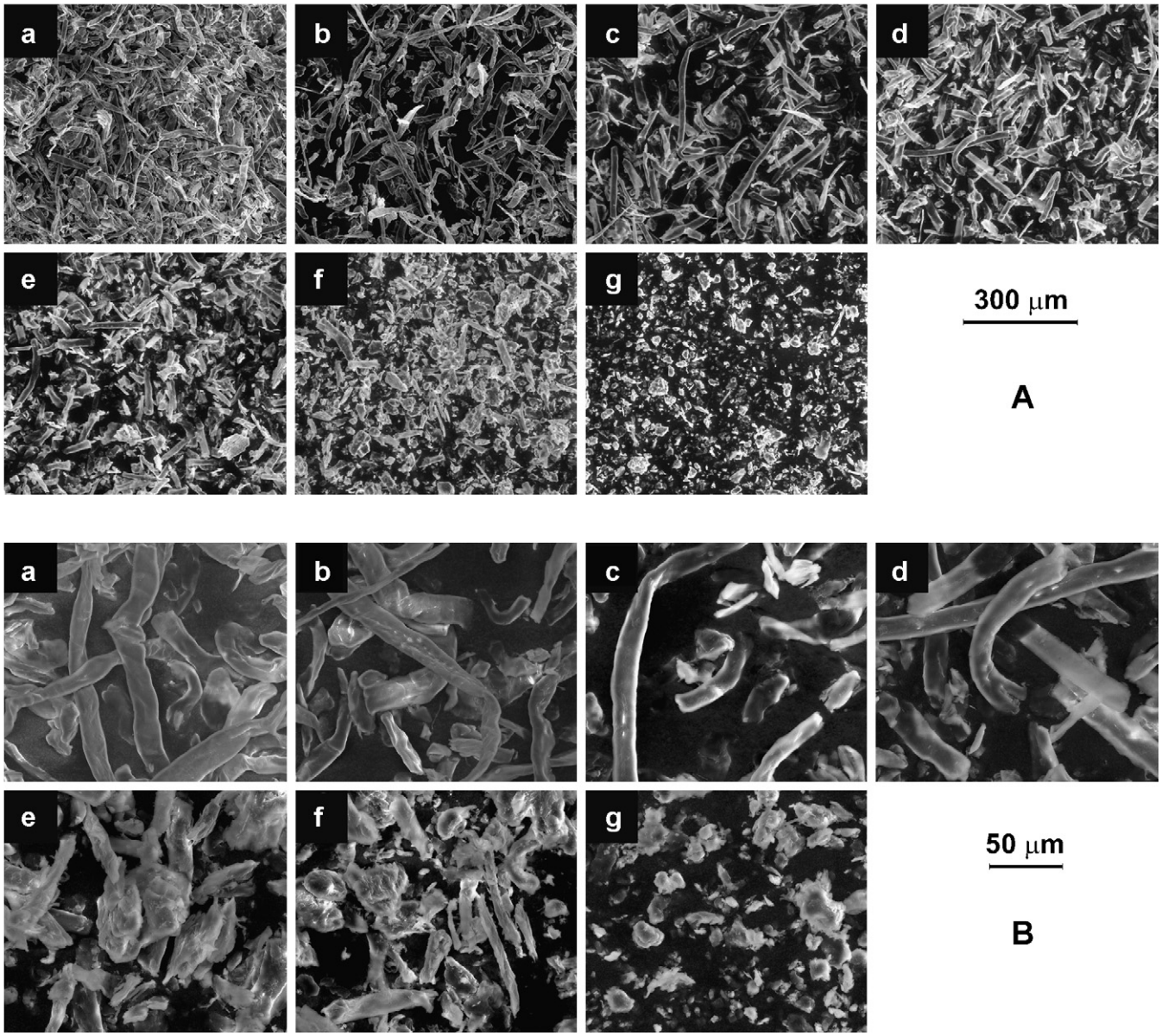

Fig. 6. SEM micrographs at lower (A) and higher magnification (B) of: (a) untreated cellulose; cellulose ball milled for: (b) 2 min, (c) 4 min, (d) 8 min, (e) 15 min, (f) 30 min, (g) 60 min.

of the fibres were evaluated, as well as the circularity (C), defined as:

$$C = 4\pi \,\text{area}/\text{perimeter}^2 \quad (13)$$

As the value of C approaches 0, it indicates an increasingly elongated shape, while a value of $C = 1$ indicates a perfect circle.

As concerning the samples ball milled for 30 and 60 min, in most cases it was not possible to recognize the original fibrous structure. Therefore, average length and diameter values, reported in Table 2, were calculated respectively as the average major and minor axis of the cellulose particles, whose shape was best fitted to an ellipse through the ImageJ software.

As already stated from a qualitative observation, the average length of the fibres strongly decreases with increasing the milling time, from an original value of about 200 μm up to a final size of about 12 μm, after 60 min ball milling. Moreover, both the aspect ratio and the circularity values clearly indicate that during the ball milling process cellulose modifies its original fibrous morphology into a quasi-circular shape. Nevertheless, it is to be remarked that during the first stages of ball milling (up to 15 min) the diameter of the fibres remains practically unchanged. Therefore it can be supposed that during this stage the main effect of the milling is the breaking of the cellulose fibres along the direction perpendicular to the fibre axis. Only after 30 min ball milling the almost complete disappearance of the fibrous structure is evidenced and the process brings to the formation of amorphous cellulose microparticles.

4. Conclusions

This paper presents a detailed analysis, performed through a multitechnique approach, of effects induced by a dry ball milling process on cellulose structure, morphology and properties.

The total energy transferred to cellulose was calculated through a kinematical model as a function of the milling time, ranging from about 102 kJ per mol of β-D-glucopyranose units (2 min milling), up to about 3060 kJ per mol of β-D-glucopyranose units (60 min ball milling).

ATR-FTIR technique allowed to qualitatively define cellulose structural changes occurred as a consequence of the ball milling process. The analysis of ATR-FTIR spectra showed a very marked intensity decrease of absorption bands centred at 1431 and 1372 cm^{-1} as a function of the ball milling time, thus indicating a progressive reduction of the cellulose crystallinity during the process.

The analysis of WAXD spectra confirmed the occurred amorphization, letting to perform a quantitative evaluation of the cellulose crystallinity index. This value decreases from 0.53 (neat cellulose) to 0.15 (after 60 min ball milling). The mean size of the cellulose crystallite domains was also calculated according to the Scherrer equation, showing a reduction from the original value of about 4.0 nm up to about 3.4 nm after 30 min ball milling.

Solid state ^{13}C CP-MAS NMR spectra of neat and ball milled samples exhibited separable resonances from crystalline and from less ordered domains for C4 and C6 atoms of anhydroglucose units. By calculating the intensity of crystalline and amorphous contribution for each resonance the NMR crystallinity index was calculated as a function of milling time, and the obtained values showed a good agreement with results obtained by WAXD analysis.

Measurements of the proton spin-lattice relaxation time in the rotating frame ($T_{1\rho}^{1H}$) showed very similar values for crystalline and amorphous domains pointing out the high efficiency of the spin-diffusion process. The calculation of the spin-diffusion path length permitted to estimate the mean dimension of crystalline and amorphous domains which resulted in accordance with WAXD data.

As an effect of the cellulose amorphization, the amount of absorbed water of cellulose conditioned at 25 °C and 50% RH increases with increasing the milling time, varying from 7.3 wt% for untreated cellulose up to 11.6 wt% for the cellulose sample ball milled for 60 min. This behaviour confirmed that water can be easily absorbed by the amorphous fraction, whereas crystalline domains are less accessible to water molecules.

Moreover, the ball milling process also influences the thermal stability of cellulose samples, slightly decreasing, especially at higher milling times, the temperature of the onset of the decomposition and the temperature corresponding to the maximum degradation rate, both being found up to 12 °C lower than the corresponding temperature values shown by untreated cellulose. Also this effect can be ascribed to the crystallinity of cellulose samples because, before the degradation process starts, a significant amount of energy is required to disrupt crystalline domains.

Another interesting consequence of the ball milling treatments is that this process strongly influences the morphology of the cellulose. The average length of the fibres decreases from an original value of about 200 μm up to a final size, after 60 min ball milling, of about 12 μm. The original fibrous morphology of the cellulose is modified to a quasi-circular shape. During the first stages of ball milling (up to 15 min) the diameter of the fibres remains practically unchanged, whereas after 30 min ball milling the almost complete disappearance of the fibrous structure is evidenced and the process brings to the formation of amorphous cellulose microparticles.

References

Abdellaoui, M., & Gaffet, E. (1995). The physics of mechanical alloying in a planetary ball mill: Mathematical treatment. *Acta Metallurgica et Materialia*, *43*, 1087–1098.

Abramoff, M. D., Magelhaes, P. J., & Ram, S. J. (2004). Image processing with ImageJ. *Biophotonics International*, *11*, 36–42.

Ago, M., Endo, T., & Hirotsu, T. (2004). Crystalline transformation of native cellulose from cellulose I to cellulose II polymorph by a ball-milling method with a specific amount of water. *Cellulose*, *11*, 163–167.

Ago, M., Endo, T., & Okajima, K. (2007). Effect of solvent on morphological and structural change of cellulose under ball-milling. *Polymer Journal*, *5*, 435–441.

Åkerholm, M., Hinterstoisser, B., & Salmén, L. (2004). Characterization of the crystalline structure of cellulose using static and dynamic FT-IR spectroscopy. *Carbohydrate Research*, *339*, 569–578.

Alexander, L. E. (1969). *X-Ray diffraction in polymer science*. New York: Wiley.

Atalla, R. H., & Van der Hart, D. L. (1984). Native cellulose: A composite of two distinct crystalline forms. *Science*, *223*, 283–285.

Avella, M., Bogoeva-Gaceva, G., Bužarovska, A., Errico, M. E., Gentile, G., & Grozdanov, A. (2007). Poly(3-hydroxybutyrate-co-3-hydroxyvalerate) based biocomposites reinforced with kenaf fibres. *Journal of Applied Polymer Science*, *104*, 3192–3200.

Avella, M., Bogoeva-Gaceva, G., Bužarovska, A., Errico, M. E., Gentile, G., & Grozdanov, A. (2008). Poly(lactic acid)-based biocomposites reinforced with kenaf fibers. *Journal of Applied Polymer Science*, *108*, 3542–3551.

Avella, M., Avolio, R., Bonadies, I., Carfagna, C., Errico, M. E., & Gentile, G. (2010). Effect of compatibilization on thermal degradation kinetics of HDPE-based composites containing cellulose reinforcements. *Journal of Thermal Analysis and Calorimetry*, *102*, 975–982.

Bai, C., Spontak, R. J., Koch, C. C., Saw, C. K., & Balik, C. M. (2000). Structural changes in poly(ethylene terephthalate) induced by mechanical milling. *Polymer*, *41*, 7147–7157.

Barsberg, S. (2010). Prediction of vibrational spectra of polysaccharides-simulated IR spectrum of cellulose based on Density Functional Theory (DFT). *Journal of Physical Chemistry B*, *114*, 11703–11708.

Burgio, N., Iasonna, A., Magini, M., Martelli, S., & Padella, F. (1991). Mechanical alloying of the Fe-Zr system. Correlation between input energy and end products. *Il Nuovo Cimento D*, *13*, 459–476.

Capitani, D., Proietti, N., Segre, A. L., & Ziarelli, F. (2002). NMR study of water-filled pores in one of the most widely used polymeric material: The paper. *Macromolecules*, *35*, 5536–5543.

Dallimore, M. P., & McCormick, P. G. (1996). Dynamics of planetary ball milling: A comparison of computer simulated processing parameters with CuO/Ni displacement reaction milling kinetics. *Materials Transactions JIM*, *37*, 1091–1098.

Evans, R., Newman, R. H., & Roick, U. C. (1995). Changes in cellulose crystallinity during kraft pulping. Comparison of infrared, x-ray diffraction and solid state NMR results. *Holzforschung*, *49*, 498–504.

Finkenstadt, V. L., & Millane, R. P. (1998). Crystal structure of valonia cellulose Iβ. *Macromolecules*, *31*, 7776–7783.

Gaffet, E. (1991). Planetary ball-milling: An experimental parameter phase diagram. *Materials Science and Engineering A*, *132*, 181–193.

Hishikawa, Y., Togawa, E., Kataoka, Y., & Kondo, T. (1999). Characterization of amorphous domains in cellulosic materials using a FTIR deuteration monitoring analysis. *Polymer*, *40*, 7117–7124.

Hori, F., Hirai, A., & Kitamaru, R. (1984). CP/MAS carbon-13 NMR study of spin relaxation phenomena of cellulose containing crystalline and noncrystalline components. *Journal of Carbohydrate Chemistry*, *3*(4), 641–662.

Hult, E.-L., Larsson, P. T., & Iversen, T. (2000). A comparative CP/MAS ^{13}C-NMR study of cellulose structure in spruce wood and kraft pulp. *Cellulose*, *7*, 35–55.

Kaplan, D. L. (1998). Introduction to biopolymers from renewable resources. In D. L. Kaplan (Ed.), *Biopolymers from renewable resources* (pp. 1–29). Berlin: Springer.

Kataoka, Y., & Kondo, T. (1998). FT-IR microscopic analysis of changing cellulose crystalline structure during wood cell wall formation. *Macromolecules*, *31*, 760–764.

Klemm, D., Philipp, B., Heinze, T., Heinze, U., & Wagenknecht, W. (1998). (1st ed.). *Comprehensive cellulose chemistry* Weinheim: Wiley-VCH.

Klemm, D., Heublein, B., Fink, H.-P., & Bohn, A. (2005). Cellulose: Fascinating biopolymer and sustainable raw material. *Angewandte Chemie International Edition*, *44*, 3358–3393.

Klemm, D., Kramer, F., Moritz, S., Lindstrom, T., Ankerfors, M., Gray, D., et al. (2011). Nanocelluloses: A new family of nature-based materials. *Angewandte Chemie International Edition*, *50*, 5438–5466.

Kocherbitov, V., Ulvenlund, S., Kober, M., Jarring, K., & Arnebrant, T. (2008). Hydration of microcrystalline cellulose and milled cellulose studied by sorption calorimetry. *Journal of Physical Chemistry B*, *112*, 3728–3734.

Langan, P., Nishiyama, Y., & Chanzy, H. (2001). X-ray Structure of Mercerized Cellulose II at 1 Å Resolution. *Biomacromolecules*, *2*, 410–416.

Larsson, P. T., Wickholm, K., & Iversen, T. (1997). A CP/MAS ^{13}C NMR investigation of molecular ordering in celluloses. *Carbohydrate Research*, *302*, 19–25.

Magini, M., & Iasonna, A. (1995). Energy transfer in mechanical alloying. *Materials Transactions JIM*, *36*, 123–133.

Magini, M., & Iasonna, A. (1996). Power measurements during mechanical milling. An experimental way to investigate the energy transfer phenomena. *Acta Materialia*, *44*, 1109–1117.

Magini, M., Iasonna, A., & Padella, F. (1996). Ball milling: An experimental support to the energy transfer evaluated by the collision model. *Scripta Materialia*, *34*, 13–19.

Magini, M., Colella, C., Iasonna, A., & Padella, F. (1998). Power measurements during mechanical milling – II. The case of "single path cumulative" solid state reaction. *Acta Materialia*, *46*, 2841–2850.

Maier, G., Zipper, P., Stubicar, M., & Schurz, J. (2005). Amorphization of different cellulose samples by ball milling. *Cellulose Chemistry and Technology*, *39*, 167–177.

Maurice, D. R., & Courtney, T. H. (1990). The physics of mechanical alloying: A first report. *Metallurgical and Materials Transactions A*, *21*, 289–302.

Murty, S., Mohan Rao, M., & Ranganathan, S. (1995). Milling maps and amorphization during mechanical alloying. *Acta Metallurgica et Materialia*, *43*, 2443–2450.

Paes, S. S., Sun, S., MacNaughtan, W., Ibbett, R., Ganster, J., Foster, T. J., et al. (2010). The glass transition and crystallization of ball milled cellulose. *Cellulose*, *17*, 693–709.

Park, S., Baker, J. O., Himmel, M. E., Parilla, P. A., & Johnson, D. K. (2010). Cellulose crystallinity index: Measurement techniques and their impact on interpreting cellulase performance. *Biotechnology for Biofuels*, *3*(10), 1–10.

Pedersoli, J. L., Jr. (2000). Effect of cellulose crystallinity on the progress of thermal oxidative degradation of paper. *Journal of Applied Polymer Science*, *78*, 61–66.

Princi, E., Vicini, S., Pedemonte, E., Gentile, G., Cocca, M., & Martuscelli, E. (2006). Synthesis and mechanical characterisation of cellulose based textiles grafted with acrylic monomers. *European Polymer Journal*, *42*, 51–60.

Schwanninger, M., Rodrigues, J. C., Pereira, H., & Hinterstoisser, B. (2004). Effects of short-time vibratory ball milling on the shape of FT-IR spectra of wood and cellulose. *Vibrational Spectroscopy*, *36*, 23–40.

Segal, L., Creely, J. J., Martin, A. E., & Conrad, C. M. (1962). An empirical method for estimating the degree of crystallinity of native cellulose using the X-ray diffractometer. *Textile Research Journal*, *29*, 786–794.

Shezad, O., Khan, S., Khan, T., & Kon Park, J. (2010). Physicochemical and mechanical characterization of bacterial cellulose produced with an excellent productivity in static conditions using a simple fed-batch cultivation strategy. *Carbohydrate Polymers*, *82*, 173–180.

Sugiyama, J., Vuong, R., & Chanzy, H. (1991). Electron diffraction study on the two crystalline phases occurring in native cellulose from an algal cell wall. *Macromolecules*, *24*, 4168–4175.

Teeäär, R., Serimaa, R., & Paakkari, T. (1987). Crystallinity of cellulose, as determined by CP/MAS NMR and XRD methods. *Polymer Bulletin*, *17*, 231–237.

Thygesen, A., Oddershede, J., Lilholt, H., Thomsen, A. B., & Ståhl, K. (2005). On the determination of crystallinity and cellulose content in plant fibres. *Cellulose*, *12*, 563–576.

Tomsic, B., Simoncic, B., Orel, B., Vilcnik, A., & Spreizer, H. (2007). Biodegradability of cellulose fabric modified by imidazolidinone. *Carbohydrate Polymers*, *69*, 478–488.

Weeber, A. W., & Bakker, H. (1988). Amorphization by ball milling. A review. *Physica B*, *153*, 93–135.

Willart, J. F., & Descamps, M. (2008). Solid state amorphization of pharmaceuticals. *Molecular Pharmaceutics*, *5*(6), 905–920.

Zhao, H., Kwak, J. H., Wang, Y., Franz, J. A., White, J. M., & Holladay, J. E. (2006). Effects of crystallinity on dilute acid hydrolysis of cellulose by cellulose ball-milling study. *Energy and Fuels*, *20*, 807–811.